

Rotational modulation of hydrogen Lyman α flux from 44 ι Bootis \star

O. Vilhu ¹, J. E. Neff ², and T. Rahunen ³

¹ Observatory and Astrophysics Laboratory, University of Helsinki, Tähtitorninmäki, SF-00130 Helsinki, Finland

² JILA, University of Colorado, Boulder, CO 80309-0440, USA

³ Sarkanniemi Oy, Tampere, Finland

Received April 22, accepted July 12, 1988

Summary. We present IUE observations that cover the entire 6.4 h orbital cycle of the late-type contact binary 44 ι Bootis. The intrinsic stellar hydrogen Lyman alpha (Ly α 1216) emission flux was determined from low-resolution IUE spectra, compensating (with specially tailored techniques) for geocoronal emission and for interstellar absorption. The variation of the stellar Ly α emission flux correlates well with the variation of the C II and C IV emission fluxes, and it shows orbital modulation in phase with the visual light curve. The uncertainty in the interstellar hydrogen column density cannot mimic the observed variation in the integrated Ly α flux, because the stellar line is very much broader than the interstellar absorption. The ratio of Ly α to C II flux (15 to 20) is similar to that observed in solar active regions, although the emission fluxes themselves are larger than in most intense solar plages. Hydrogen Ly α emission is thus one of the most important cooling channels in the outer atmosphere of 44 ι Boo. We obtained a high-resolution spectrum of the Ly α line between orbital phases 0.0 and 0.6. The integrated flux in the observed high-resolution Ly α profile is consistent with the fluxes determined using low-resolution spectra, and the composite profile indicates that both components of this binary have equally active chromospheres and transition regions. Each component would therefore have almost equal “dynamo numbers”.

Key words: magnetic activity – chromospheres – Lyman alpha emission – ultraviolet spectroscopy – contact binaries

1. Introduction

The atmospheres of late-type stars consist of relatively cool photospheres, warm chromospheres, and hot coronae. The chromosphere and corona are separated by a thin transition region, in which the temperature changes abruptly from about 7000 K to several million K.

It has been shown on the basis of IUE and EINSTEIN observations that the emission fluxes in various chromospheric lines (Ca II H and K, Mg II h and k, O I), in transition region lines

(C IV, Si IV, N V), and in the coronal soft X rays are well correlated (Ayres, et al, 1981; Oranje, et al, 1982; Pallavicini et al., 1982; Walter, et al, 1982; Vilhu 1984). In particular, with increasing stellar activity the transition region line fluxes and the X-ray flux increase more rapidly than the chromospheric emission: $f(\text{TR}) - f(\text{Chr})^\alpha$ and $f(X) \sim f(\text{Chr})^\beta$, where $\alpha = 1.5$ and $\beta = 2-3$. So far, correlations of this type have been established on a broad statistical basis for G and K dwarfs and G giants. Differences from these relationships exist for special groups of stars. For instance, contact binaries are somewhat underactive in X rays and Mg II emission, as compared to the transition region line emission (Vilhu and Walter, 1987).

The Lyman alpha line at 1216 Å (Ly α) plays a crucial role in the energetic relationship between the chromospheres and coronae of cool stars. Unfortunately, the possible correlation between the Ly α line flux and other chromospheric and transition region line fluxes has not yet been investigated, mainly because the very strong Ly α line is generally overexposed on all IUE short wavelength (SWP) spectra taken with exposure times long enough to make other interesting spectral features, such as C IV 1550 and C II 1335, visible. In addition, the stellar emission in low-resolution spectra is severely contaminated by scattered solar Ly α emission from the geocoronal environment of the IUE satellite. Further, interstellar absorption can remove a significant fraction of the intrinsic stellar flux from the line.

Nevertheless, it is extremely important that we determine the intrinsic strength of the Ly α emission and possible correlations it might have with other emissions from the outer atmosphere. Since the major constituent of the chromospheric plasma is hydrogen, emission of its principal resonance line must play a critical role in the global energy balance, particularly at the interface between the chromosphere and corona, where the hydrogen is strongly ionizing (Hammer et al, 1982; Hammer and Linsky, 1985). The Ly α emission flux from the Sun is approximately as large as the total emission from the solar transition region in all other lines. According to empirical models of the solar chromosphere, most of the Ly α radiation originates from a thin layer at the foot of the transition region (Vernazza, et al, 1981). It is not known, however, whether the Ly α emitting layer is thick enough that the radiative loss balances the dissipation of mechanical or magnetic energy flux from below or instead balances excess energy transported downward from the corona, perhaps by thermal conduction or in the enthalpy and potential energy content of downflowing gas.

The existence of any correlation of the flux of Ly α with the flux of other lines from the chromosphere, transition region, or

Send offprint requests to: O. Vilhu

\star Based on observations with the International Ultraviolet Explorer (IUE) obtained at the Villafranca satellite tracking station of the European Space Agency and at NASA/Goddard Space Flight Center.

Table 1. IUE observations of 44 *i* Boo on 28 June and 6 July 1986. The $L\alpha$ fluxes are corrected for the geocoronal emission and interstellar absorption (using $N_{\text{H}} = 10^{18} \text{ cm}^{-2}$)

SWP	RES	Start (UT)	Exp. (min)	JD mid 2446610+	Phase	Line fluxes $10^{-12} \text{ erg s}^{-1} \text{ cm}^{-2}$		
						$L\alpha$	C II	C IV
28564	Low	16:23	10	0.186	0.56	9.3	0.77	1.65
28565	Low	17:12	15	0.215	0.66	17.7	0.96	1.89
28566	Low	17:59	15	0.255	0.81	16.7	1.05	1.89
28567	Low	18:46	15	0.287	0.93	13.7	0.73	1.53
25568	Low	19:34	15	0.320	0.05	16.5	0.89	1.84
28569	Low	20:22	15	0.353	0.17	20.5	1.17	2.62
28570	Low	21:25	15	0.397	0.34	17.3	0.90	2.14
28571	Low	22:35	15	0.446	0.52	13.5	0.69	1.26
28625	High	19:52	249	8.419	0.92–0.57	17.2	^a	^a

^a Not measurable in high-resolution spectrum

corona, or with magnetic field strength and surface area filling factors (Saar, 1987) should shed light on the energy balance of the outer atmosphere.

Nearby contact binaries are good targets to study the $L\alpha$ emission, because they are expected to have strong emission and because their emission lines are rotationally broadened so that interstellar absorption does not remove a large fraction of the total flux. In addition, the short periods of contact binaries allow an orbital modulation study to be made. It is possible to perform a simultaneous study of the $L\alpha$ line and many chromospheric and transition region emission lines from the contact binary system 44 *i* Boo with short SWP exposures (which would not be saturated at Lyman alpha). In addition, 44 *i* Boo is bright enough that a high resolution Lyman alpha spectrum can be obtained (although over a large spread in orbital phases), allowing an important check on the techniques used to remove the effects of geocoronal emission and interstellar absorption from the low-resolution spectra.

In this paper we study the orbital modulation of the $L\alpha$ emission from 44 *i* Boo, one of the brightest contact binary systems. We then compare this emission with other far-ultraviolet emission line fluxes. We compare these results with solar active regions and with other active stars, especially W UMa, the first contact binary studied in Lyman alpha (Rucinski et al, 1985).

2. Observations

44 *i* Bootis (HD 133640; SAO 45357) is a contact binary at a distance of 12 pc. It has been well studied with the IUE (Rucinski and Vilhu, 1983) and with the EINSTEIN (Craddock and Dupree, 1984) and EXOSAT (Vilhu and Heise, 1986) observatories. Optical studies are complicated by a visual companion that lies a few arc seconds away and is in an astrometric orbit with the period of 246 years. The G0 spectral type companion is brighter ($V = 5.3$) than the contact binary ($V = 6.1$; $B - V = 0.85$). However, the visual companion is not expected to contribute appreciably to the UV or X-ray emission, because it is a slowly rotating star, and thus inactive, and the surface fluxes of the chromospheric and coronal emission of 44 *i* Boo (including the visual companion) are not noticeably higher than those of similar contact binaries.

The amplitudes of the radial velocity variations of 44 *i* Boo are $K1 = 115 \text{ km s}^{-1}$ and $K2 = 231 \text{ km s}^{-1}$ (Batten, et al, 1978). The

mass ratio is $M2/M1 = 0.50$, and the orbital inclination $i = 77^\circ$ (Rucinski, 1973). The ephemeris of light minimum given in Vilhu and Heise (1986) needs to be corrected by 0.015 days to be consistent with the July 1986 photometry of Al-Naimiy et al. (1986). We used the orbital ephemeris $\text{JD}(\text{min}) = 2439852.5053$ and the orbital period of 0.2678159 days.

The low-resolution SWP observations were performed on 28 June 1986 during a contiguous US2 + ESA double shift covering roughly one orbital cycle. A high-resolution spectrum was obtained on 6 July 1986, with an exposure begun at about primary minimum lasting until secondary minimum (one half of the orbital cycle). A log of these observations is given in Table 1.

We used the IUE Fine Error Sensor (FES) to obtain the visual light curve of the contact system. Table 2 gives times and corresponding phases, the FES counts, and the magnitudes $V(i + \text{comp})$ when the 5.3 mag visual companion is included and $V(i)$ when it is subtracted.

Table 2. The FES light curve of 44 *i* Boo on 28 June 1986

UT	Phase	Counts	$V(i + \text{comp})^a$	$V(i)^b$	$f_{\text{bol}}(i)^c$
16:43	0.596	22858	4.95	6.35	0.93
17:30	0.718	24147	4.86	6.05	1.23
18:18	0.843	23864	4.88	6.11	1.17
19:05	0.965	22071	5.00	6.54	0.79
19:53	0.089	23183	4.93	6.28	0.99
20:41	0.218	24303	4.85	6.02	1.27
20:54	0.252	24411	4.84	5.99	1.30
21:01	0.270	24693	4.83	5.96	1.34
21:23	0.327	24159	4.85	6.02	1.27
21:56	0.413	23409	4.88	6.11	1.17
22:33	0.509	22279	4.93	6.28	0.99

^a V magnitude including the visual companion.

^b V magnitude of the contact binary only.

^c In units of $10^{-7} \text{ erg s}^{-1} \text{ cm}^{-2}$, computed from $f(\text{bol}) = 2.7 \cdot 10^{-5} \cdot 10^{-0.4(V+BC)}$ using $BC = -0.2$.

3. Determination of line fluxes

3.1. Measurement of line fluxes

All reduction and analysis of the IUE observations was performed using software at the Colorado Regional Data Analysis Facility (RDAF). After applying the standard flux calibration to one-dimensional extracted spectra, the Ly α (1216 Å), C II (1335 Å), and C IV (1550 Å) fluxes were determined by fitting a gaussian emission profile to the spectral line and a quadratic function to the local background. The integrated line fluxes for C II and C IV, listed in Table 1, require no further correction. The Lyman alpha fluxes of Table 1 have been corrected for the excess emission due to geocoronal emission, and for the fraction of the stellar emission absorbed by neutral hydrogen in the interstellar medium. Both of these effects were expressly accounted for in order to determine the intrinsic stellar flux (see Sects. 3.2 and 3.3).

3.2. Correction for geocoronal emission

Solar Ly α emission is resonantly scattered into the line of sight by hydrogen in the “geocorona”. The major axis of the elliptical large aperture is oriented roughly perpendicular to the dispersion in low-resolution spectra and roughly parallel to it in high-resolution spectra. From the geosynchronous orbital position of the IUE spacecraft, geocoronal emission is seen from all directions, therefore uniformly illuminating the aperture. The intensity of the two-dimensional (spatial and spectral dimensions) geocoronal profile varies with the angle between the line of sight and the sun, the angle between the line of sight and the Earth, and the intrinsic variability of the solar Ly α (Clarke, 1982), but the shape of the profile is due solely to instrumental factors. This profile shows light loss near the edge of the aperture due to the point-spread function of the telescope, and is roughly flat across the center of the aperture.

We subtracted the geocoronal profile from the low-resolution SWP images using the method developed by Neff et al. (1986). The correction procedure operates on the standard line-by-line (ELBL) files, which include a series of spatially resolved spectra. These spatially resolved spectra are treated as an “image” of the aperture. Geocoronal emission is present throughout the aperture, while the stellar emission is confined to the center of the aperture. We fitted a model profile perpendicular to the dispersion (i.e. in the spatial dimension) at each wavelength within the aperture. This profile was subtracted from each spatial slice to produce a corrected line-by-line file, which may then be co-added with standard IUE software to yield the stellar spectrum with the geocoronal background removed.

The geocoronal model profile consists of gaussian wings fit to the outer portion of the aperture (where light loss is significant) and a linear interpolation across the center of the aperture (the central 11 lines in the line-by-line spectrum). We therefore use the information within the aperture but outside the region that contains stellar emission to determine the intensity level of the geocoronal emission. Thus, this procedure will work with any spectrum in the IUE archive. This profile has proven to give a satisfactory fit in cases when only the geocorona was observed (sky background or quasar spectra, Neff et al. 1986). Table 3 gives the integrated Ly α emission line fluxes before and after the geocoronal subtraction for all our SWP low resolution observations. For this particular set of observations the stellar emission was strong and exposure times short, so the geocoronal contribution was relatively small.

Table 3. The Ly α fluxes before and after the geocoronal correction was applied (in units of 10^{-12} erg s $^{-1}$ cm $^{-2}$). The fraction of the stellar emission absorbed by the interstellar medium is also given (assuming $N_{\text{H}} = 10^{18}$ cm $^{-2}$)

SWP	Before	After	Fraction absorbed by the ISM
28564	20.9	7.3	0.22
28565	23.6	14.2	0.20
28566	20.4	13.7	0.18
28567	14.7	10.8	0.21
28568	15.0	12.9	0.22
28569	19.4	16.8	0.18
28570	17.0	14.2	0.18
28571	11.7	10.4	0.23

Table 4. Mean fractional and surface fluxes of 44 *t* Boo^a

	$f/f(\text{bol})$ 10^{-5}	Surface flux 10^5 ergs s $^{-1}$ cm $^{-2}$
Ly α	16.5 ± 2.0	65 ± 8
C II	0.90 ± 0.15	3.7 ± 0.6
C IV	1.86 ± 0.35	7.7 ± 1.4

^a Mean of 8 exposures

We compared our results with those of Rucinski, Vilhu, and Whelan (1985), who extracted the geocoronal contribution with different techniques for the prototype contact binary WUMa. Two SWP images (8639 and 8641) were used. For $f(\text{Ly}\alpha)/f(\text{bol})$ Rucinski et al. found values 3.4 E-5 and 3.1 E-5, respectively. Our geocoronal subtraction, instead, gave values 12.7 E-5 and 16.7 E-5 for SWP 8639 and SWP 8641, respectively. The difference is significant, by a factor of 4 to 5! Previous IUE studies have shown that the fractional chromospheric and transition region line fluxes $f/f(\text{bol})$ of 44 *t* Boo and WUMa are of the same magnitude (see e.g. Rucinski and Vilhu 1983). For Ly α , one should expect the same. This is consistent with our values (see Table 4 for 44 *t* Boo). We believe on our values also because the geocoronal contribution in the 44 *t* Boo spectra is small and because our high-resolution spectrum is clearly consistent with the inferred Ly α fluxes.

3.3. Correction for interstellar absorption

Because the Ly α line profile is not resolved in low-resolution observations, the only way to estimate how much of the stellar flux is removed by interstellar absorption is to model both the stellar emission and interstellar absorption profiles. The only observational constraint available in the low-resolution spectra is the total integrated flux in the earth-received profile. Other parameters of the model must be constrained with prior knowledge or else varied between their reasonable limits. We used the method described by Rucinski et al. (1985), who argued that since the

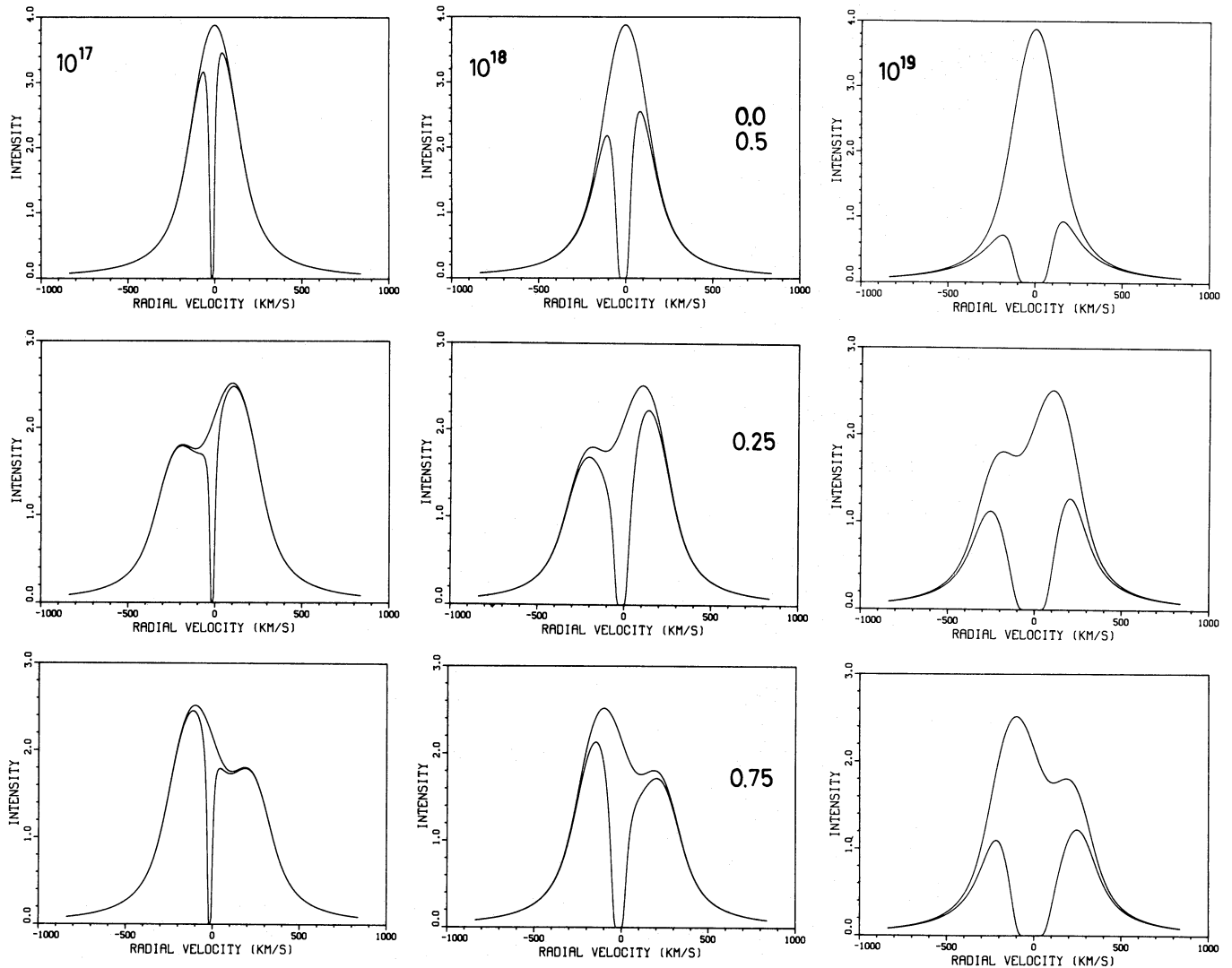


Fig. 1. Model profiles for the Ly α emission line for 44*i* Boo. The models include the rotational and intrinsic broadenings of both components and the absorption due to interstellar hydrogen. Models were computed for three hydrogen column densities N_{H} (10^{17} , 10^{18} , and 10^{19} atoms cm^{-2}) and for three orbital phases. The intensity scale is arbitrary, and the wavelength (horizontal scale) (in km s^{-1}) has its origin at the binary's center of mass. The two curves at each panel are without and with the interstellar absorption, respectively

stellar profiles of contact binaries are very broad (rapid rotators), the interstellar absorption is not extremely large unless the interstellar hydrogen column density is greater than 10^{19} cm^{-2} . For narrow-lined stars the situation is quite different, as even very small column densities cause the interstellar absorption to affect the entire stellar emission profile.

Figure 1 shows a set of theoretical Ly α emission line profiles for 44*i* Boo computed with the code kindly provided by S.M. Rucinski. This code was described by Rucinski et al, (1985) in their similar study of W UMa. For 44*i* Boo we used the mass ratio 0.5, the orbital inclination 77 degrees, and the contact fill-out factor 0.9 (as given in Rucinski, 1973). We used different interstellar hydrogen column densities, although the most probable value is less than 10^{18} cm^{-2} (Vilhu and Heise, 1986). In particular, Bruhweiler and Kondo (1982) derive a column density 10^{18} cm^{-2} for a white dwarf W 1346 that lies at roughly the same distance and galactic longitude (13 pc and 67° ; 44*i* Boo lies at 12 pc and at longitude of 80°), but at smaller galactic latitude (-9°), than 44*i* Boo (57°).

The system radial velocity of 44*i* Boo, with respect to the sun, is 3.4 km s^{-1} (Batten et al, 1978). The long astrometric orbit does not affect this value significantly. Using the flow vector for the local interstellar medium (l, b, v) = ($25^{\circ}, 10^{\circ}, -28 \text{ km s}^{-1}$) from Crutcher (1982), the radial velocity of the interstellar gas in the direction of 44*i* Boo is -12.6 km s^{-1} . The observations of Böhm-Vitense (1981 a) and Bruhweiler and Vidal-Madjar (1986) support in general the use of the Crutcher- vector given above. In this way we deduce that the interstellar gas is moving with respect to 44*i* Boo with a velocity of approximately -16 km s^{-1} . This values was used in modelling the interstellar absorption.

Figure 2 shows the fraction of the total stellar Ly α emission flux that is absorbed as a function of the interstellar hydrogen column density N_{H} and orbital phase. Typically, when N_{H} is less than 10^{18} cm^{-2} , the absorbed fraction is less than 25%, and it varies with the orbital phase by less than 10%. The fluxes listed in Table 1 were derived assuming $N_{\text{H}} = 10^{18} \text{ cm}^{-2}$. In Table 3, we list the factor used to correct each of the observed spectra.

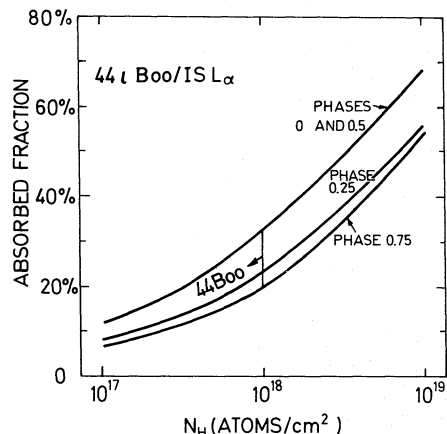


Fig. 2. The fraction of stellar Ly α emission that is absorbed as a function of the interstellar hydrogen column density N_H and orbital phase

4. Results

Figure 3 shows the light curves for the Ly α 1216, C II 1335, and C IV 1550 emission lines, normalized to their maximum values. The Lyman alpha fluxes were corrected for geocoronal emission and for interstellar absorption. The FES counts (representing the V light curve) are plotted together with a synthetic visual (5500 Å) light curve computed with the code kindly provided by S.M. Rucinski. This code was described by Rucinski (1973). Between orbital phases 0.0 and 0.5 the emission line and visual light curves are very similar ($f/f(\text{bol}) = \text{const}$). However, the line fluxes (especially C IV) seem to be lower between phases 0.5 and 0.0. If true, this indicates that the transition region on the phase 0.75 side of the system is fainter than that on the phase 0.25 side. However, the observations between phases 0.5 and 0.0 were made at higher radiation levels and are of poorer quality than those observed later, when the radiation was negligible.

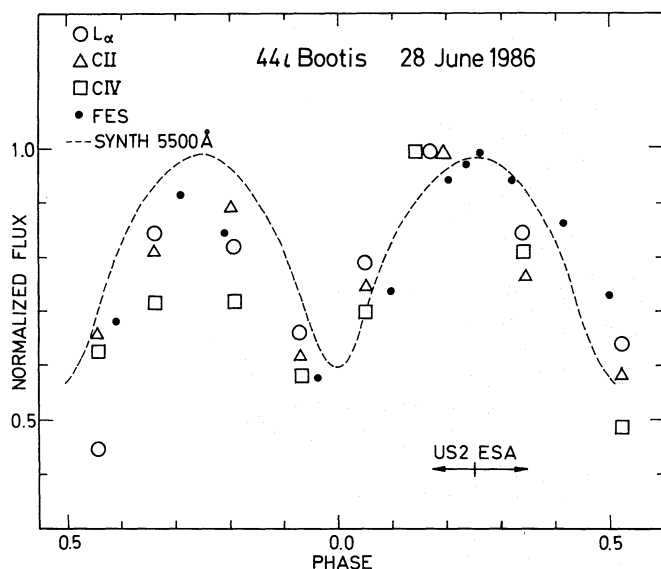


Fig. 3. The stellar Ly α , C II 1335, and C IV 1550 emission line light curves of 44 ι Boo. The visual points from the IUE Fine Error Sensor (FES) and the computed synthetic visual light curve (SYNTH) are shown for comparison

The high-resolution spectrum SWP 28625 obtained about a week later between phases 0 and 0.5 provides us with a means to verify our Ly α correction procedures. The spectrum is shown in Fig. 4. In this high-resolution spectrum the narrow geocoronal emission (labelled) is clearly seen, mostly masking the underlying interstellar absorption. However, the broad stellar wings are visible. For comparison, a theoretical profile is shown. This profile was computed with $N_H = 10^{18} \text{ cm}^{-2}$ and a flux mean between phases 0.92 and 0.57, weighting the profiles of different phases with the low-resolution Ly α fluxes (after the geocoronal subtraction). The total flux in the theoretical stellar emission profile (without interstellar absorption) is $17.2 \cdot 10^{-12} \text{ erg s}^{-1} \text{ cm}^{-2}$. This value is somewhat uncertain ($\pm 20\%$), since no actual fit with the observed wings was attempted. However, the fit is reasonable, and the total Ly α flux used is quite compatible with the mean low-resolution flux between phases 0 and 0.5.

When computing the interstellar absorption profile we used the asymptotic attenuation factor ($\exp(-\text{const } N_H (\lambda - \lambda_0)^{-2})$), instead of the correct factor $\exp(-\text{const } N_H H(a, u))$, where $H(a, u)$ is the Voigt function, as used by McClintock et al. (1978). Comparing with Fig. 4 of McClintock et al., we find an excellent agreement, since the interstellar hydrogen absorption is very strong. The depth of the small absorption feature at the wavelength of the Deuterium absorption in Fig. 4 is also consistent with the McClintock et al. results for N_H around 10^{18} cm^{-2} and $D/H = 1.8 \text{ E-}5$ (see their Fig. 4). Unfortunately, our spectrum does not allow a direct determination of the D/H ratio.

5. Discussion and summary

The symmetry of the high-resolution Ly α profile and the lack of any clear rotational modulation of $f/f(\text{bol})$ imply that both components of the 44 ι Boo system must have similar chromospheres and transition regions. This should be expected, because both components have almost equal effective temperatures and apparently equal angular velocities. To a zeroth approximation, each component would therefore have equal “dynamo numbers”.

The classical theory of contact binaries assumes “a common convective envelope” where both stars are embedded. However, more developed theories deviate from thermal equilibrium, producing quite unequal convective zones for the component stars (see for example Rahunen, 1981, 1982; Rahunen and Vilhu, 1982). If the chromospheric and transition region line fluxes are indicative of magnetic activity, then the dynamo power of the components should be equal, and the physical properties of the dynamo layers (such as temperature, density, rotation, differential rotation, turbulent velocities, etc.) should be equal as a consequence. However, as pointed by Vilhu and Heise (1986), because contact binaries are close to the observed saturation limits of all chromospheric and transition region indicators, this test is very insensitive to the dynamo-related parameters.

Table 4 gives the mean values for the emission line fluxes over the phase duration of about one orbital cycle. The surface fluxes (at the star) were computed from the fractional fluxes $f/f(\text{bol})$, multiplying them by the bolometric surface flux σT_{eff}^4 using $T_{\text{eff}} = 5200 \text{ K}$, which follows from the calibration by Böhm-Vitense (1981 b) at $B - V = 0.85$. The Ly α surface flux is very close to the Mg II 2800 emission line flux and somewhat smaller than the soft X-ray flux between 0.1 keV and 4.5 keV. All of these fluxes are also close to the observed saturation levels at $B - V = 0.85$: about 10^6 , 10^7 , and $10^{7.5} \text{ ergs s}^{-1} \text{ cm}^{-2}$ for C IV, Mg II, and soft X rays,

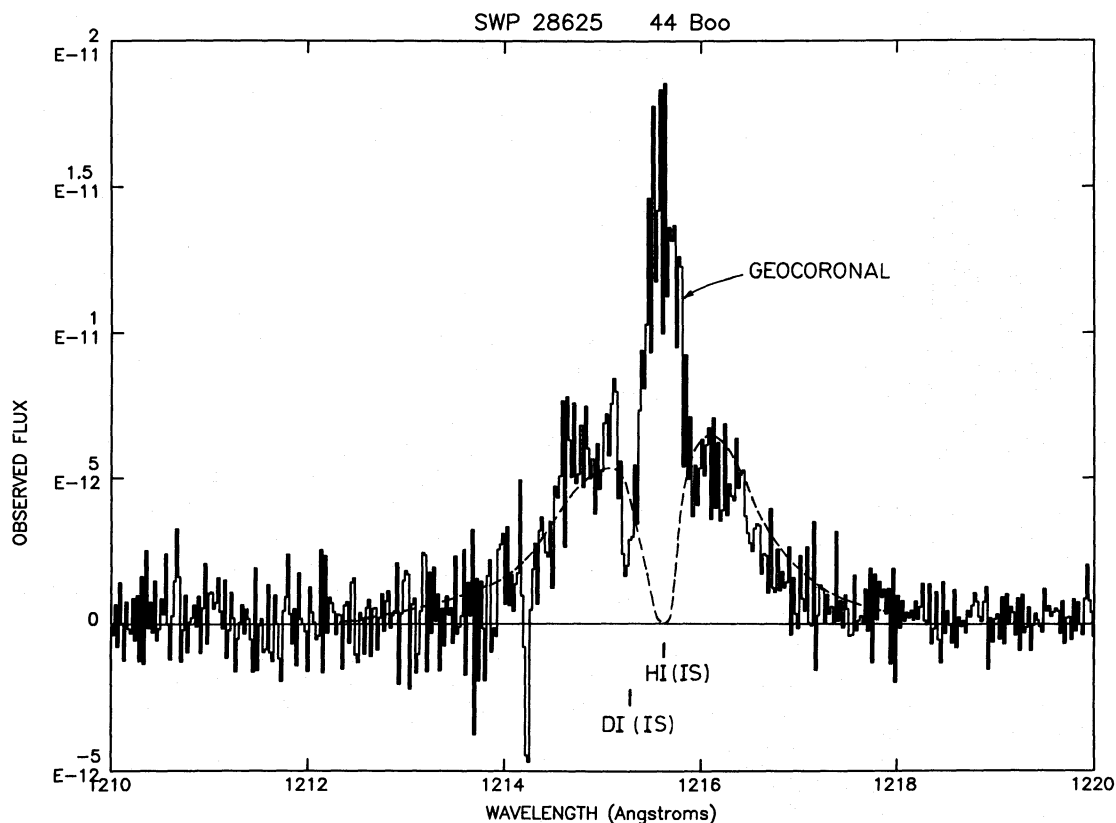


Fig. 4. The high-resolution Ly α spectrum of 44 Boo obtained 6 July 1986, between orbital phases 0.92–0.57 (flux in units of $\text{erg cm}^{-2} \text{s}^{-1}$). The theoretical profile is shown by the dashed line. The geocoronal emission is clearly visible inside the broad stellar emission wings. The position of the interstellar neutral hydrogen and deuterium absorptions are marked

respectively (Vilhu and Walter, 1987). Hence, Ly α is an important cooling agent in 44 Boo.

The total C II and Ly α intensities of solar active regions are correlated, and a linear relation $F(\text{Ly}\alpha) = 25 F(\text{C II})$ for a sample of active regions follows from Schrijver et al. (1985). From Table 4 we find for 44 Boo $F(\text{Ly}\alpha) = (18 \pm 6) F(\text{C II})$, quite consistent with the solar active region data. We note, however, that the absolute values of the surface fluxes in 44 Boo are much larger, indicating higher surface coverage of magnetic field than in solar plages. In the most intense solar active region studied by Schrijver et al. $F(\text{Ly}\alpha) = 2.5 \cdot 10^6 \text{ erg s}^{-1} \text{ cm}^{-2}$, compared with the mean value $6.5 \cdot 10^6 \text{ erg s}^{-1} \text{ cm}^{-2}$ for 44 Boo.

Acknowledgements. We are very grateful to Slavek Rucinski for providing us with his contact binary computer codes. This work was supported by NASA grant NAG 5-82 to the University of Colorado. The data analysis was performed at the Colorado Regional Data Analysis Facility, which is supported by NASA grant NAG 5-26409 to the University of Colorado.

References

- Al-Naimiy et al.: 1986, IBVS 2956
 Ayres, T.R., Marstad, N.C., Linsky, J.L.: 1981, *Astrophys. J.* **247**, 545
 Batten, A.H., Flechter, J.M., Mann, P.: 1978, *Publ. Dominion Astrophys. Obs.* XV, No. 5
 Böhm-Vitense, E.: 1981a, *Astrophys. J.* **244**, 504
 Böhm-Vitense, E.: 1981b, *Ann. Rev. Astron. Astrophys.* **19**, 295
 Bruhweiler, F.C., Kondo, Y.: 1982, *Astrophys. J.* **259**, 232
 Bruhweiler, F.C., Vidal-Madjar, A.: 1986, in *Exploring the Universe with the IUE Satellite*, ed. Y. Kondo, Reidel, Dordrecht, p. 467
 Clarke, J.T.: 1982, *Astrophys. J.* **263**, L105
 Cruddace, R.G., Dupree, A.K.: 1984, *Astrophys. J.* **277**, 263
 Crutcher, R.M.: 1982, *Astrophys. J.* **254**, 82
 Hammer, R., Linsky, J.L., Endler, F.: 1982, in *Advances in Ultraviolet Astronomy: Four Years of IUE Research*, eds. Y. Kondo, J. Mead, R. Chapman, NASA CP-2238, p. 268
 Hammer, R., Linsky, J.L.: 1985, ESA SP-218, p. 25
 McClintock, W., Henry, R.C., Linsky, J.L., Moos, H.W.: 1978, *Astrophys. J.* **225**, 465
 Neff, J.E., Linsky, J.L., Landsman, W.B., Carpenter, K.G.: 1986, in *New Insights in Astrophysics: 8 Years of UV Astronomy with IUE*, ESA-SP 263, p. 669
 Oranje, B.J., Zwaan, C., Middelkoop, F.: 1982, *Astron. Astrophys.* **110**, 30
 Pallavicini, R., Golub, L., Rosner, R., Vaiana, G.S., Ayres, T., Linsky, J.L.: 1981, *Ap. J.* **248**, 279
 Rahunen, T.: 1981, *Astron. Astrophys.* **102**, 81
 Rahunen, T.: 1982, *Astron. Astrophys.* **109**, 66
 Rahunen, T., Vilhu, O.: 1982, in *Binary and Multiple Stars as Tracers of Stellar Evolution*, eds. Z. Kopal, J. Rahe, Reidel, Dordrecht, p. 289
 Rucinski, S.M.: 1973, *Acta Astron.* **23**, 79

- Rucinski, S.M., Vilhu, O.: 1983, *Monthly Notices Roy. Astron. Soc.* **202**, 1221
- Rucinski, S.M., Vilhu, O., Whelan, J.A.J.: 1985, *Astron. Astrophys.* **143**, 153
- Saar, S.H.: 1987, PhD thesis, University of Colorado, Boulder
- Schrijver, C.J., Zwaan, C., Maxson, C.W., Noyes, R.W.: 1985, *Astron. Astrophys.* **149**, 123
- Vernazza, J.E., Avrett, E.H., Loeser, R.: 1981, *Astrophys. J. Suppl.* **45**, 635
- Vilhu, O.: 1984, *Astron. Astrophys.* **133**, 117
- Vilhu, O.: 1987, in *Cool Stars, Stellar Systems, and the Sun*, eds. J.L. Linsky, R.E. Stencel, Springer, Berlin, Heidelberg, New York, p. 110
- Vilhu, O., Heise, J.: 1986, *Astrophys. J.* **311**, 937
- Vilhu, O., Walter, F.M.: 1987, *Astrophys. J.* **321**, 958
- Walter, F.M., Basri, G.S., Laurent, R.: 1982, in *Advances in Ultraviolet Astronomy: Four Years of IUE Research*, eds. Y. Kondo, J.M. Mead, R.D. Chapman, NASA CP-2238, p. 566